Hindawi Publishing Corporation
Mathematical Problems in Engineering
Volume 2010, Article ID 782457, 13 pages
doi:10.1155/2010/782457

Research Article

Control of Limit Cycle Oscillations of a Two-Dimensional Aeroelastic System

M. Ghommem, A. H. Nayfeh, and M. R. Hajj

Department of Engineering Science and Mechanics, Virginia Polytechnic Institute and State University, Blacksburg, VA 24061, USA

Correspondence should be addressed to M. R. Hajj, mhajj@vt.edu

Received 19 August 2009; Accepted 3 November 2009

Academic Editor: José Balthazar

Linear and nonlinear static feedback controls are implemented on a nonlinear aeroelastic system that consists of a rigid airfoil supported by nonlinear springs in the pitch and plunge directions and subjected to nonlinear aerodynamic loads. The normal form is used to investigate the Hopf bifurcation that occurs as the freestream velocity is increased and to analytically predict the amplitude and frequency of the ensuing limit cycle oscillations (LCO). It is shown that linear control can be used to delay the flutter onset and reduce the LCO amplitude. Yet, its required gains remain a function of the speed. On the other hand, nonlinear control can be effciently implemented to convert any subcritical Hopf bifurcation into a supercritical one and to significantly reduce the LCO amplitude.

1. Introduction

The response of an aeroelastic system is governed by a combination of linear and nonlinear dynamics. When combined, the nonlinearities (geometric, inertia, free-play, damping, and/or aerodynamics) lead to different behavior [1–3], including multiple equilibria, bifurcations, limit cycles, chaos, and various types of resonances (internal and super/subharmonic) [4]. A generic nonlinear system that has been used to characterize aeroelastic behavior and dynamic instabilities is a two-dimensional rigid airfoil undergoing pitch and plunge motions [5, 6]. As the parameters of this system (e.g., freestream velocity) are varied, changes may occur in its behavior. Of particular interest is its response around a bifurcation point. Depending on the relative magnitude and type of nonlinearity, the bifurcation can be of the subcritical or supercritical type. Hence, one needs to consider the combined effects of all nonlinearities to predict the system's response. Furthermore, the nonlinearities provide an opportunity to implement a combination of linear and nonlinear control strategies to delay the occurrence

of the bifurcation (i.e., increase the allowable flight speed) and avoid catastrophic behavior of the system (subcritical Hopf bifurcation) by suppressing or even alleviating the large-amplitude LCO and eliminating LCO that may take place at speeds lower than the nominal flutter speed.

Different methods have been proposed to control bifurcations and achieve desirable nonlinear effects in complex systems. Abed and Fu [7, 8] proposed a nonlinear feedback control to suppress discontinuous bifurcations of fixed points, such as subcritical Hopf bifurcations, which can result in loss of synchronism or voltage collapse in power systems. For the pitch-plunge airfoil, Strganac et al. [9] used a trailing edge flap to control a two-dimensional nonlinear aeroelastic system. They showed that linear control strategies may not be appropriate to suppress large-amplitude LCO and proposed a nonlinear controller based on partial feedback linearization to stabilize the LCO above the nominal flutter velocity. Librescu et al. [10] implemented an active flap control for 2D wing-flap systems operating in an incompressible flow field and exposed to a blast pulse and demonstrated its performances in suppressing flutter and reducing the vibration level in the subcritical flight speed range. Kang [11] developed a mathematical framework for the analysis and control of bifurcations and used an approach based on the normal form to develop a feedback design for delaying and stabilizing bifurcations. His approach involves a preliminary state transformation and center manifold reduction.

In this work, we present a methodology to convert subcritical bifurcations of aeroelastic systems into supercritical bifurcations. This methodology involves the following steps: (i) reduction of the dynamics of the system into a one-dimensional dynamical system using the method of multiple scales and then (ii) designing a nonlinear feedback controller to convert subcritical to supercritical bifurcations and reduce the amplitude of any ensuing LCO.

2. Representation of the Aeroelastic System

The aeroelastic system, considered in this work, is modeled as a rigid wing undergoing two-degree-of-freedom motions, as presented in Figure 1. The wing is free to rotate about the elastic axis (pitch motion) and translate vertically (plunge motion). Denoting by h and α the plunge deflection and pitch angle, respectively, we write the governing equations of this system as [4, 9]

$$\begin{pmatrix} m_T & m_W x_\alpha b \\ m_W x_\alpha b & I_\alpha \end{pmatrix} \begin{pmatrix} \ddot{h} \\ \ddot{\alpha} \end{pmatrix} + \begin{pmatrix} c_h & 0 \\ 0 & c_\alpha \end{pmatrix} \begin{pmatrix} \dot{h} \\ \dot{\alpha} \end{pmatrix} + \begin{pmatrix} k_h(h) & 0 \\ 0 & k_\alpha(\alpha) \end{pmatrix} \begin{pmatrix} h \\ \alpha \end{pmatrix} = \begin{pmatrix} -L \\ M \end{pmatrix}, \tag{2.1}$$

where m_T is the total mass of the wing and its support structure, m_W is the wing mass alone, I_α is the mass moment of inertia about the elastic axis, b is the half chord length, $x_\alpha = r_{cg}/b$ is the nondimensionalized distance between the center of mass and the elastic axis, c_h and c_α are the plunge and pitch structural damping coefficients, respectively, L and M are the aerodynamic lift and moment about the elastic axis, and k_h and k_α are the structural stiffnesses for the plunge and pitch motions, respectively. These stiffnesses are approximated

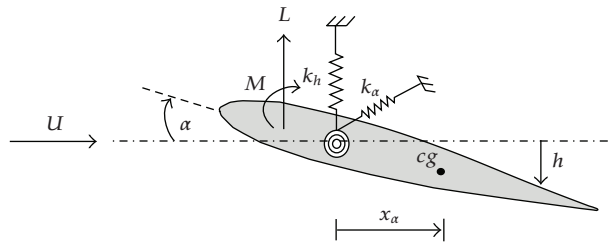

Figure 1: Sketch of a two-dimensional airfoil.

in polynomial form by

$$k_\alpha(\alpha) = k_{\alpha 0} + k_{\alpha 1}\alpha + k_{\alpha 2}\alpha^2 + \cdots,$$
$$k_h(h) = k_{h0} + k_{h1}h + k_{h2}h^2 + \cdots. \tag{2.2}$$

The aerodynamic loads are evaluated using a quasi-steady approximation with a stall model [9] and written as

$$L = \rho U^2 b c_{l_\alpha}\left(\alpha_{\text{eff}} - c_s\alpha_{\text{eff}}^3\right),$$
$$M = \rho U^2 b^2 c_{m_\alpha}\left(\alpha_{\text{eff}} - c_s\alpha_{\text{eff}}^3\right), \tag{2.3}$$

where U is the freestream velocity, c_{l_α} and c_{m_α} are the aerodynamic lift and moment coefficients, and c_s is a nonlinear parameter associated with stall. The effective angle of attack due to the instantaneous motion of the airfoil is given by [9]

$$\alpha_{\text{eff}} = \alpha + \frac{\dot{h}}{U} + \left(\frac{1}{2} - a\right)b\frac{\dot{\alpha}}{U}, \tag{2.4}$$

where a is the nondimensionalized distance from the midchord to the elastic axis.

For the sake of simplicity, we define the state variables

$$\mathbf{Y} = \begin{pmatrix} Y_1 \\ Y_2 \\ Y_3 \\ Y_4 \end{pmatrix} = \begin{pmatrix} h \\ \alpha \\ \dot{h} \\ \dot{\alpha} \end{pmatrix}, \tag{2.5}$$

and write the equations of motion in the form

$$\dot{\mathbf{Y}} = F(\mathbf{Y}, U), \tag{2.6}$$

Table 1: System variables.

$d = m_T I_\alpha - m_W^2 x_\alpha^2 b^2$
$k_1 = (I_\alpha \rho b c_{l_\alpha} + m_W x_\alpha \rho b^3 c_{m_\alpha})/d$
$k_2 = -(m_W x_\alpha \rho b^2 c_{l_\alpha} + m_T \rho b^2 c_{m_\alpha})/d$
$c_1 = [I_\alpha (c_h + \rho U b c_{l_\alpha}) + m_W x_\alpha \rho U b^3 c_{m_\alpha}]/d$
$c_2 = [I_\alpha \rho U b^2 c_{l_\alpha}(1/2 - a) - m_W x_\alpha b c_{l_\alpha} + m_W x_\alpha \rho U b^4 c_{m_\alpha}(1/2 - a)]/d$
$c_3 = [-m_W x_\alpha b(c_h + \rho U b c_{l_\alpha}) - m_T x_\alpha \rho U b^2 c_{m_\alpha}]/d$
$c_4 = [m_T(c_\alpha - \rho U b^3 c_{m_\alpha}(1/2 - a)) - m_W x_\alpha \rho U b^3 c_{l_\alpha}(1/2 - a)]/d$
$p_\alpha(\mathbf{Y}) = -m_W x_\alpha b k_\alpha(\mathbf{Y})/d$
$q_\alpha(\mathbf{Y}) = m_T k_\alpha(\mathbf{Y})/d$
$p_h(\mathbf{Y}) = I_\alpha k_h(\mathbf{Y})/d$
$q_h(\mathbf{Y}) = -m_W x_\alpha b k_h(\mathbf{Y})/d$
$g_{NL1}(\mathbf{Y}) = (c_s \rho U^2 b)(c_{l_\alpha} I_\alpha + m_W x_\alpha b^2 c_{m_\alpha}) \alpha_{\text{eff}}^3(\mathbf{Y})/d$
$g_{NL2}(\mathbf{Y}) = -(c_s \rho U^2 b^2)(c_{l_\alpha} m_W x_\alpha + m_T c_{m_\alpha}) \alpha_{\text{eff}}^3(\mathbf{Y})/d$

where

$$F(\mathbf{Y}, U) = \begin{pmatrix} Y_3 \\ Y_4 \\ -p_h(Y_1)Y_1 - \left(k_1 U^2 + p_\alpha(Y_2)\right)Y_2 - c_1 Y_3 - c_2 Y_4 + g_{NL1}(Y) \\ -q_h(Y_1)Y_1 - \left(k_2 U^2 + q_\alpha(Y_2)\right)Y_2 - c_3 Y_3 - c_4 Y_4 + g_{NL2}(Y) \end{pmatrix}. \tag{2.7}$$

The set of new variables that are used in (2.7) in terms of physical parameters is provided in Table 1. The original system, (2.6), is then rewritten as

$$\dot{\mathbf{Y}} = A(U)\mathbf{Y} + Q(\mathbf{Y}, \mathbf{Y}) + C(\mathbf{Y}, \mathbf{Y}, \mathbf{Y}), \tag{2.8}$$

where $Q(\mathbf{Y}, \mathbf{Y})$ and $C(\mathbf{Y}, \mathbf{Y}, \mathbf{Y})$ are, respectively, the quadratic and cubic vector functions of the state variables collected in the vector $\mathbf{Y}$.

To determine the system's stability, we consider the linearized governing equations, which are written in a first-order differential form as

$$\dot{\mathbf{Y}} = A(U)\mathbf{Y}, \tag{2.9}$$

where

$$A(U) = \begin{pmatrix} 0 & 0 & 1 & 0 \\ 0 & 0 & 0 & 1 \\ -\dfrac{I_\alpha k_{h0}}{d} & -\left(k_1 U^2 - \dfrac{m_W x_\alpha b k_{\alpha 0}}{d}\right) & -c_1 & -c_2 \\ \dfrac{m_W x_\alpha b k_{h0}}{d} & -\left(k_2 U^2 + \dfrac{m_T k_{\alpha 0}}{d}\right) & -c_3 & -c_4 \end{pmatrix}. \tag{2.10}$$

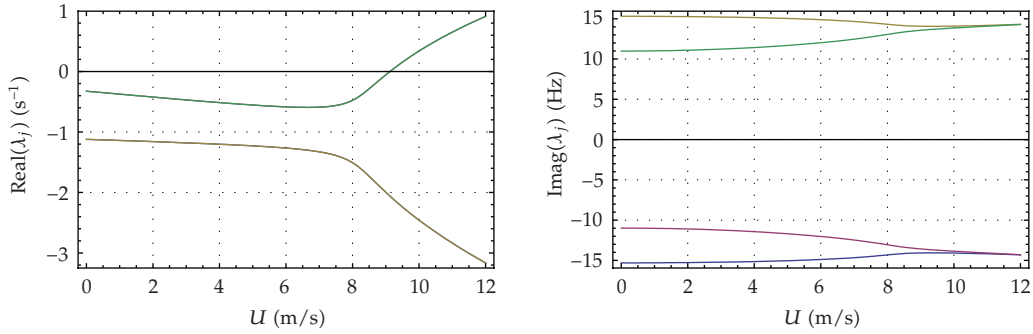

Figure 2: Variations of (a) damping (Real(λ_j)) and (b) frequencies (Imag(λ_j)) with the freestream velocity U.

The 4×4 matrix $A(U)$ has a set of four eigenvalues, $\{\lambda_j,\ j = 1, 2, \ldots, 4\}$. These eigenvalues determine the stability of the trivial solution of (2.6). If the real parts of all of the λ_j are negative, the trivial solution is asymptotically stable. On the other hand, if the real part of one or more eigenvalues is positive, the trivial solution is unstable. The flutter speed U_f, for which one or more eigenvalues have zero real parts, corresponds to the onset of linear instability. For the specific values given in [9], Figures 2(a) and 2(b) show, respectively, variations of the real and imaginary parts of the λ_j with U, which, respectively, correspond to the damping and frequencies of the plunge and pitch motions. We note that the damping of two modes becomes positive at $U_f = 9.1242\,\mathrm{m/s}$, which corresponds to the flutter speed at which the aeroelastic system undergoes a Hopf bifurcation.

3. Static Feedback Control

To manage the Hopf bifurcation and achieve desirable nonlinear dynamics, we follow Nayfeh and Balachandran [12] and use a static feedback control. To the system given by (2.6), we add a static feedback $\mathbf{u}(\mathbf{Y})$, which includes linear, $L_u\mathbf{Y}$, quadratic $Q_u(\mathbf{Y}, \mathbf{Y})$, and cubic $C_u(\mathbf{Y}, \mathbf{Y}, \mathbf{Y})$ components; that is,

$$\mathbf{u}(\mathbf{Y}) = L_u\mathbf{Y} + Q_u(\mathbf{Y}, \mathbf{Y}) + C_u(\mathbf{Y}, \mathbf{Y}, \mathbf{Y}). \tag{3.1}$$

Hence, the controlled system takes the form

$$\dot{\mathbf{Y}} = F(\mathbf{Y}, U) + \mathbf{u}(\mathbf{Y}). \tag{3.2}$$

3.1. Normal Form of Hopf Bifurcation

To compute the normal form of the Hopf bifurcation of (3.2) near $U = U_f$, we follow Nayfeh and Balachandran [12] and introduce a small nondimensional parameter ϵ as a book keeping

parameter. Defining the velocity perturbation as a ratio of the flutter speed $\sigma_U U_f$, we write $U = U_f + \epsilon^2 \sigma_U U_f$ and seek a third-order approximate solution of (3.2) in the form

$$\mathbf{Y}(t, \sigma_U, \sigma_\alpha, \sigma_h) = \epsilon \mathbf{Y}_1(T_0, T_2) + \epsilon^2 \mathbf{Y}_2(T_0, T_2) + \epsilon^3 \mathbf{Y}_3(T_0, T_2) + \cdots, \tag{3.3}$$

where the time scales $T_m = \epsilon^m t$. In terms of these scales, the time derivative d/dt is written as

$$\frac{d}{dt} = \frac{\partial}{\partial T_0} + \epsilon^2 \frac{\partial}{\partial T_2} + \cdots = D_0 + \epsilon^2 D_2 + \cdots. \tag{3.4}$$

Scaling L_u as $\epsilon^2 L_u$, substituting (3.3) and (3.4) into (3.2), and equating coefficients of like powers of ϵ, we obtain

Order (ϵ),

$$D_0 \mathbf{Y}_1 - A(U_f)\mathbf{Y}_1 = 0, \tag{3.5}$$

Order (ϵ^2),

$$D_0 \mathbf{Y}_2 - A(U_f)\mathbf{Y}_2 = Q(\mathbf{Y}_1, \mathbf{Y}_1) + Q_u(\mathbf{Y}_1, \mathbf{Y}_1), \tag{3.6}$$

Order (ϵ^3),

$$\begin{aligned} D_0 \mathbf{Y}_3 - A(U_f)\mathbf{Y}_3 = {} & -D_2 \mathbf{Y}_1 + \sigma_U B \mathbf{Y}_1 + L_u \mathbf{Y}_1 + 2[Q(\mathbf{Y}_1, \mathbf{Y}_2) + Q_u(\mathbf{Y}_1, \mathbf{Y}_2)] \\ & + C(\mathbf{Y}_1, \mathbf{Y}_1, \mathbf{Y}_1) + C_u(\mathbf{Y}_1, \mathbf{Y}_1, \mathbf{Y}_1), \end{aligned} \tag{3.7}$$

where

$$B = -2k_1 U_f^2 I_1 - 2k_2 U_f^2 I_2, \quad I_1 = \begin{pmatrix} 0 & 0 & 0 & 0 \\ 0 & 0 & 0 & 0 \\ 0 & 1 & 0 & 0 \\ 0 & 0 & 0 & 0 \end{pmatrix}, \quad I_2 = \begin{pmatrix} 0 & 0 & 0 & 0 \\ 0 & 0 & 0 & 0 \\ 0 & 0 & 0 & 0 \\ 0 & 1 & 0 & 0 \end{pmatrix}. \tag{3.8}$$

The general solution of (3.5) is the superposition of four linearly independent solutions corresponding to the four eigenvalues: two of these eigenvalues have negative real parts and the other two are purely imaginary $(\pm i\omega)$. Because the two solutions corresponding to the two eigenvalues with negative real parts decay as $T_0 \to \infty$, we retain only the nondecaying solutions and express the general solution of the first-order problem as

$$\mathbf{Y}_1(T_0, T_2) = \eta(T_2)\mathbf{p}e^{i\omega T_0} + \overline{\eta}(T_2)\overline{\mathbf{p}}e^{-i\omega T_0}, \tag{3.9}$$

where $\eta(T_2)$ is determined by imposing the solvability condition at the third-order level and $\mathbf{p}$ is the eigenvector of $A(U_f)$ corresponding to the eigenvalue $i\omega$; that is,

$$A(U_f)\mathbf{p} = i\omega \mathbf{p}. \tag{3.10}$$

Substituting (3.9) into (3.6) yields

$$D_0\mathbf{Y}_2 - A(U_f)\mathbf{Y}_2 = [Q(\mathbf{p},\mathbf{p}) + Q_u(\mathbf{p},\mathbf{p})]\eta^2 e^{2i\omega T_0} + 2[Q(\mathbf{p},\overline{\mathbf{p}}) + Q_u(\mathbf{p},\overline{\mathbf{p}})]\eta\overline{\eta} + [Q(\overline{\mathbf{p}},\overline{\mathbf{p}}) + Q_u(\overline{\mathbf{p}},\overline{\mathbf{p}})]\overline{\eta}^2 e^{-2i\omega T_0}. \tag{3.11}$$

The solution of (3.11) can be written as

$$\mathbf{Y}_2 = (\zeta_2 + \zeta_{2u})\eta^2 e^{2i\omega T_0} + 2(\zeta_0 + \zeta_{0u})\eta\overline{\eta} + \left(\overline{\zeta}_2 + \overline{\zeta}_{2u}\right)\overline{\eta}^2 e^{-2i\omega T_0}, \tag{3.12}$$

where

$$\begin{aligned} [2i\omega I - A(U_f)]\zeta_2 &= Q(\mathbf{p},\mathbf{p}), \qquad [2i\omega I - A(U_f)]\zeta_{2u} = Q_u(\mathbf{p},\mathbf{p}), \\ A(U_f)\zeta_0 &= -Q_u(\mathbf{p},\overline{\mathbf{p}}), \qquad A(U_f)\zeta_{0u} = -Q_u(\mathbf{p},\overline{\mathbf{p}}). \end{aligned} \tag{3.13}$$

Substituting (3.9) and (3.12) into (3.7), we obtain

$$\begin{aligned} D_0\mathbf{Y}_3 - A(U_f)\mathbf{Y}_3 = -\Big[& D_2\eta\mathbf{p} - (\sigma_U B + L_u)\eta\mathbf{p} \\ & - (4Q(\mathbf{p},\zeta_0) + 2Q(\overline{\mathbf{p}},\zeta_2) \\ & + 3C(\mathbf{p},\mathbf{p},\overline{\mathbf{p}}) + 4Q_u(\mathbf{p},\zeta_0) + 2Q_u(\overline{\mathbf{p}},\zeta_2) \\ & + 3C_u(\mathbf{p},\mathbf{p},\overline{\mathbf{p}}) + 4Q(\mathbf{p},\zeta_{0u}) + 2Q(\overline{\mathbf{p}},\zeta_{2u}))\eta^2\overline{\eta}\Big] e^{i\omega T_0} + \text{cc} + \text{NST}, \end{aligned} \tag{3.14}$$

where cc stands for the complex conjugate of the preceding terms and NST stands for terms that do not produce secular terms. We let $\mathbf{q}$ be the left eigenvector of $A(U_f)$ corresponding to the eigenvalue $i\omega$; that is,

$$A(U_f)^T\mathbf{q} = i\omega\mathbf{q}. \tag{3.15}$$

We normalize it so that $\mathbf{q}^T\mathbf{p} = 1$. Then, the solvability condition requires that terms proportional to $e^{i\omega T_0}$ in (3.14) be orthogonal to $\mathbf{q}$. Imposing this condition, we obtain the following normal of the Hopf bifurcation:

$$D_2\eta = \widehat{\beta}\eta + \widehat{\Lambda}\eta^2\overline{\eta}, \tag{3.16}$$

where

$$\widehat{\beta} = \beta + \beta_u, \tag{3.17}$$

with

$$\beta = \mathbf{q}^T \sigma_U B \mathbf{p}, \qquad \beta_u = \mathbf{q}^T L_u \mathbf{p},$$
$$\widehat{\Lambda} = \Lambda + \Lambda_u, \tag{3.18}$$

with

$$\begin{aligned}\Lambda &= 4\mathbf{q}^T Q(\mathbf{p}, \zeta_0) + 2\mathbf{q}^T Q(\overline{\mathbf{p}}, \zeta_2) + 3\mathbf{q}^T C(\mathbf{p}, \mathbf{p}, \overline{\mathbf{p}}),\\ \Lambda_u &= 4\mathbf{q}^T Q_u(\mathbf{p}, \zeta_0) + 2\mathbf{q}^T Q_u(\overline{\mathbf{p}}, \zeta_2) + 3\mathbf{q}^T C_u(\mathbf{p}, \mathbf{p}, \overline{\mathbf{p}})\\ &\quad + 4\mathbf{q}^T Q(\mathbf{p}, \zeta_{0u}) + 2\mathbf{q}^T Q(\overline{\mathbf{p}}, \zeta_{2u}).\end{aligned} \tag{3.19}$$

Letting $\eta = (1/2)a\exp(i\theta)$ and separating the real and imaginary parts in (3.16), we obtain the following alternate normal form of the Hopf bifurcation:

$$\dot{a} = \widehat{\beta}_r a + \frac{1}{4}\widehat{\Lambda}_r a^3, \tag{3.20}$$

$$\dot{\theta} = \widehat{\beta}_i + \frac{1}{4}\widehat{\Lambda}_i a^2, \tag{3.21}$$

where $(\cdot)_r$ and $(\cdot)_i$ stand for the real and imaginary parts, respectively, a is the amplitude and $\dot{\theta}$ is the frequency of the oscillatory motion associated with the Hopf bifurcation.

We note that, because the a component is independent of θ, the system's stability is reduced to a one-dimensional dynamical system given by (3.20). Assuming that $\widehat{\Lambda}_r \neq 0$, a admits three steady-state solutions, namely,

$$a = 0, \quad a = \pm\sqrt{\frac{-4\widehat{\beta}_r}{\widehat{\Lambda}_r}}. \tag{3.22}$$

The trivial fixed point of (3.20) corresponds to the fixed point $(0,0)$ of (3.2), and a nontrivial fixed point (i.e., $a \neq 0$) of (3.20) corresponds to a periodic solution of (3.2). The origin is asymptotically stable when $\widehat{\beta}_r < 0$, unstable when $\widehat{\beta}_r > 0$, unstable when $\widehat{\beta}_r = 0$ and $\widehat{\Lambda}_r > 0$, and asymptotically stable when $\widehat{\beta}_r = 0$ and $\widehat{\Lambda}_r < 0$. On the other hand, the nontrivial fixed points exist when $-\widehat{\beta}_r\widehat{\Lambda}_r > 0$. They are stable when $\widehat{\beta}_r > 0$ and $\widehat{\Lambda}_r < 0$ (supercritical Hopf bifurcation) and unstable when $\widehat{\beta}_r < 0$ and $\widehat{\Lambda}_r > 0$ (subcritical Hopf bifurcation). We note that a stable nontrivial fixed point of (3.20) corresponds to a stable periodic solution of (3.2). Likewise, an unstable nontrivial fixed point of (3.20) corresponds to an unstable periodic solution of (3.2).

Therefore, to delay the occurrence of Hopf bifurcation (i.e., stabilize the aeroelastic system at speeds higher than the flutter speed), one needs to set the real part of $\widehat{\beta}$ to a negative value by appropriately managing the linear control represented by L_u in (3.2). To eliminate subcritical instabilities and limit LCO amplitudes to small values at speeds higher than the flutter speed (supercritical Hopf bifurcation which is a favorable instability for such

systems), the nonlinear feedback control given by $Q_u(\mathbf{Y},\mathbf{Y}) + C_u(\mathbf{Y},\mathbf{Y},\mathbf{Y})$ should be chosen so that $\text{Real}(\Lambda + \Lambda_u) < 0$.

3.2. Case Study

To demonstrate the linear and nonlinear control strategies, we consider an uncontrolled case (i.e., $\mathbf{u}(\mathbf{Y}) = 0$) in which only the pitch structural nonlinearity is taken into account; that is, $k_{h1} = k_{h2} = c_s = 0$, $k_{\alpha 1} = 9.9967$, and $k_{\alpha 2} = 167.685$. The hysteretic response as a function of the freestream velocity, obtained through the numerical integration of (2.6) for these parameters, is presented in Figure 3. The onset of flutter takes place at $U_f = 9.1242\,\text{m/s}$ and is characterized by a jump to a large-amplitude LCO when transitioning through the Hopf bifurcation. As the speed is increased beyond the flutter speed, the LCO amplitudes of both of the pitch and plunge motions increase. Furthermore, LCO take place at speeds lower than U_f if the disturbances to the system are sufficiently large. Clearly, this configuration exhibits a subcritical instability ($\text{Real}(\Lambda) > 0$).

For linear control, we consider the matrix L_u defined in (3.2) in the form of

$$L_u = \begin{pmatrix} -k_l & 0 & 0 & 0 \\ 0 & 0 & 0 & 0 \\ 0 & 0 & 0 & 0 \\ 0 & 0 & 0 & 0 \end{pmatrix}, \tag{3.23}$$

where k_l is the linear feedback control gain. Then, for the specific values of the system parameters given in [9], we obtain

$$\widehat{\beta} = \left(0.433891\sigma_U U_f - 0.110363k_l\right) + \imath\left(0.323942\sigma_U U_f - 0.303804k_l\right). \tag{3.24}$$

To guarantee damped oscillations of the airfoil at speeds higher than the flutter speed, one needs to set k_l to a value such that $\text{Real}(\widehat{\beta}) < 0$. Using a gain of 10, we plot in Figure 4 the plunge and pitch displacements for a freestream velocity of $U = 10\,\text{m/s}$ with and without linear control. Clearly, linear control damps the LCO of the uncontrolled system. We note that, by increasing the linear feedback control gain k_l, the amplitudes of pitch and plunge decay more rapidly.

Although linear control is capable of delaying the onset of flutter in terms of speed and reducing the LCO amplitude, the system would require higher gains at higher speeds. Furthermore, it maintains its subcritical response. To overcome these difficulties and convert the subcritical instability to a supercritical one, we introduce the following nonlinear feedback control law:

$$\mathbf{u}^T = -\left(k_{\text{nl1}} \;\; k_{\text{nl2}} \;\; k_{\text{nl3}} \;\; k_{\text{nl4}}\right)\dot{\alpha}^3, \tag{3.25}$$

where the k_{nli} are the nonlinear feedback control gains. For the specific airfoil's geometry given in [9], we obtain

$$\widehat{\Lambda}_r = 0.866899 - \left(132.844k_{\text{nl1}} + 13.3643k_{\text{nl2}} + 2.9858k_{\text{nl3}} + 1.32415k_{\text{nl4}}\right). \tag{3.26}$$

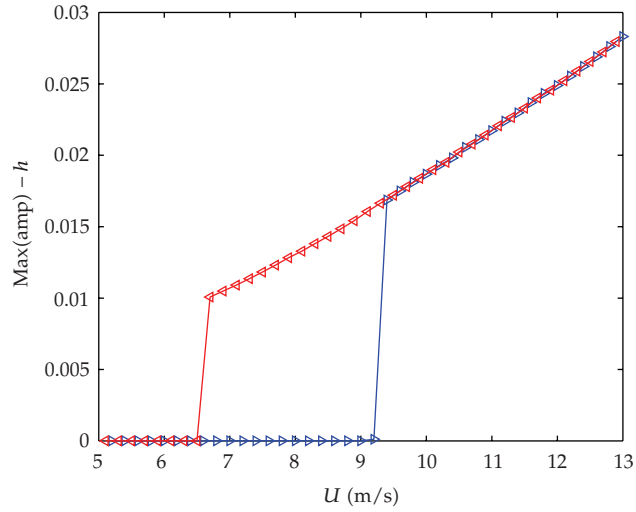

(a) Plunge motion

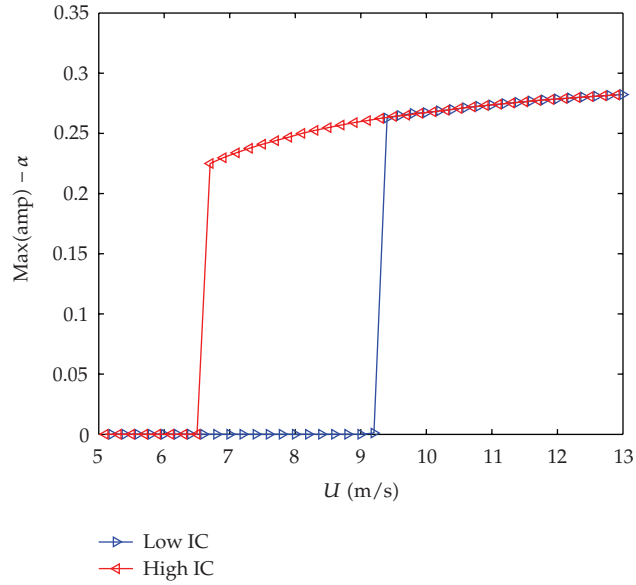

(b) Pitch motion

Figure 3: Hysteretic response of the aeroelastic system (subcritical instability). The steady-state amplitudes are plotted as a function of U.

This equation shows that applying gain to the plunge displacement is more effective than applying it to the pitch displacement or plunge velocity or pitch velocity.

The subcritical instability takes place for positive values of $\widehat{\Lambda}_r$. As such it can be eliminated by forcing $\widehat{\Lambda}_r$ to be negative. This can be achieved by using nonlinear control gains $k_{\text{nl1}} = 0.02$ ($k_{\text{nl2}} = k_{\text{nl3}} = k_{\text{nl4}} = 0$). The results are presented in Figure 5. The subcritical Hopf bifurcation at U_f observed in Figure 3 has been transformed into the supercritical Hopf bifurcation of Figure 5. A comparison of the two figures shows that the unstable limit

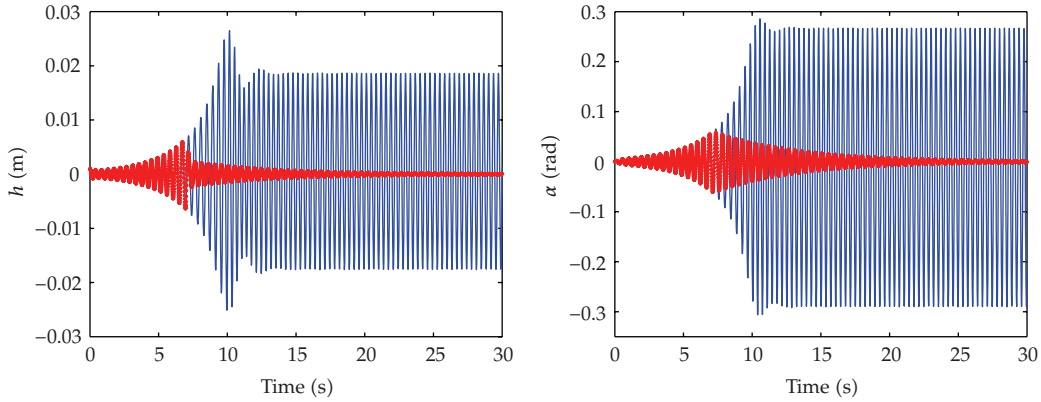

(a) Plunge motion (b) Pitch motion

Figure 4: Measured pitch and plunge responses:: −, without linear control, ∗, with linear control.

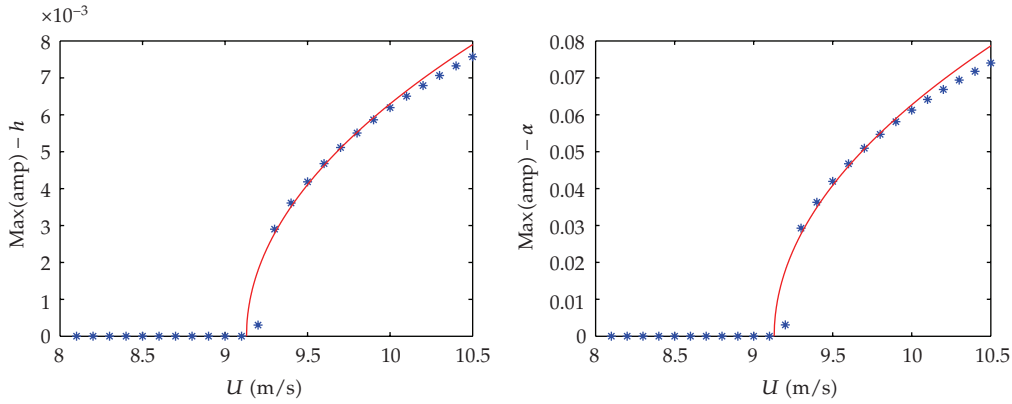

(a) Plunge motion (b) Pitch motion

Figure 5: LCO amplitudes of plunge and pitch motions (controlled configuration): −, analytical prediction, ∗, numerical integration.

cycles observed over the freestream speed between $U = 6.5\,\mathrm{m/s}$ and $U = 9.12\,\mathrm{m/s}$ have been eliminated. Furthermore, the exponentially growing oscillations predicted by the linear model are limited to a periodic solution whose amplitude increases slowly with increasing freestream velocity. Moreover, increasing the value of k_{nl1} reduces the amplitude of the limit cycles created due to Hopf bifurcation.

In order to check the accuracy of the analytical formulation given by the normal form in predicting the amplitude of LCO near the Hopf bifurcation, we consider the first-order solution given by (3.9). The amplitude of plunge and pitch LCO, A_h and A_α, respectively, are given by

$$A_h = a\sqrt{\mathbf{p1}_r^2 + \mathbf{p1}_i^2},$$
$$A_\alpha = a\sqrt{\mathbf{p2}_r^2 + \mathbf{p2}_i^2}, \tag{3.27}$$

where $\mathbf{pj}_r$ and $\mathbf{pj}_i$ denote the real and imaginary parts of the jth component of the vector $\mathbf{p}$, respectively. In Figures 5(a) and 5(b), we plot the LCO amplitudes for both pitch and plunge motions obtained by integrating the original system and those predicted by the normal form. The results show good agreement in the LCO amplitudes only near the bifurcation.

4. Conclusions

Linear and nonlinear controls are implemented on a rigid airfoil undergoing pitch and plunge motions. The method of multiple scales is applied to the governing system of equations to derive the normal form of the Hopf bifurcation near the flutter onset. The linear and nonlinear parameters of the normal form are used to determine the stability characteristics of the bifurcation and efficiency of the linear and nonlinear control components. The results show that linear control can be used to delay the flutter onset and dampen LCO. Yet, its required gains remain a function of the speed. On the other hand, nonlinear control can be efficiently implemented to convert subcritical to supercritical Hopf bifurcations and to significantly reduce LCO amplitudes.

Acknowledgment

M. Ghommem is grateful for the support from the Virginia Tech Institute for Critical Technology and Applied Science (ICTAS) Doctoral Scholars Program.

References

[1] E. H. Dowell and D. Tang, "Nonlinear aeroelasticity and unsteady aerodynamics," *AIAA Journal*, vol. 40, no. 9, pp. 1697–1707, 2002.

[2] A. Raghothama and S. Narayanan, "Non-linear dynamics of a two-dimensional air foil by incremental harmonic balance method," *Journal of Sound and Vibration*, vol. 226, no. 3, pp. 493–517, 1999.

[3] L. Liu, Y. S. Wong, and B. H. K. Lee, "Application of the centre manifold theory in non-linear aeroelasticity," *Journal of Sound and Vibration*, vol. 234, no. 4, pp. 641–659, 2000.

[4] H. C. Gilliatt, T. W. Strganac, and A. J. Kurdila, "An investigation of internal resonance in aeroelastic systems," *Nonlinear Dynamics*, vol. 31, no. 1, pp. 1–22, 2003.

[5] B. H. K. Lee, L. Y. Jiang, and Y. S. Wong, "Flutter of an airfoil with a cubic restoring force," *Journal of Fluids and Structures*, vol. 13, no. 1, pp. 75–101, 1999.

[6] C. C. Chabalko, M. R. Hajj, D. T. Mook, and W. A. Silva, "Characterization of the LCO response behaviors of the NATA model," in *Proceedings of the 47th AIAA/ASME/ASCE/AHS/ASC Structures, Structural Dynamics and Materials Conference*, vol. 5, pp. 3196–3206, Newport, RI, USA, May 2006, AIAA paper no.2006-1852.

[7] E. H. Abed and J.-H. Fu, "Local feedback stabilization and bifurcation control. I. Hopf bifurcation," *Systems & Control Letters*, vol. 7, no. 1, pp. 11–17, 1986.

[8] E. H. Abed and J.-H. Fu, "Local feedback stabilization and bifurcation control. II. Stationary bifurcation," *Systems & Control Letters*, vol. 8, no. 5, pp. 467–473, 1987.

[9] T. W. Strganac, J. Ko, D. E. Thompson, and A. J. Kurdila, "Identification and control of limit cycle oscillations in aeroelastic systems," in *Proceedings of the 40th AIAA/ASME/ASCE/AHS/ASC Structrures, Structural Dynamics, and Materials Conference and Exhibit*, vol. 3, pp. 2173–2183, St. Louis, Mo, USA, April 1999, AIAA paper no. 99-1463.

[10] L. Librescu, S. Na, P. Marzocca, C. Chung, and M. K. Kwak, "Active aeroelastic control of 2-D wing-flap systems operating in an incompressible flowfield and impacted by a blast pulse," *Journal of Sound and Vibration*, vol. 283, no. 3–5, pp. 685–706, 2005.

[11] W. Kang, "Bifurcation control via state feedback for systems with a single uncontrollable mode," *SIAM Journal on Control and Optimization*, vol. 38, no. 5, pp. 1428–1452, 2000.

[12] A. H. Nayfeh and B. Balachandran, *Applied Nonlinear Dynamics. Analytical, Computational, and Experimental Methods*, Wiley Series in Nonlinear Science, John Wiley & Sons, New York, NY, USA, 1995.